RSC Sustainability

ROYAL SOCIETY OF CHEMISTRY

PAPER

View Article Online
View Journal | View Issue

Cite this: *RSC Sustainability*, 2024, **2**, 2005

Synthesis and characterization of magnetic carbonaceous materials from bamboo waste and investigation of their adsorption capability for cesium ions

Fumihiko Ogata,[a] Noriaki Nagai,[a] Taiki Ogawa,[a] Yugo Uematsu,[a] Chalermpong Saenjum,[bc] Shigeharu Tanei[d] and Naohito Kawasaki *[ae]

In this work, we prepared a series of magnetic carbonaceous materials (CB200F, CB400F, CB600F, CB800F, and CB1000) from waste bamboo (RB) for the removal of cesium ions from water. Physicochemical properties such as pH_{pzc}, specific surface area, and surface functional groups of the prepared adsorbents were evaluated and their cesium ion adsorption capability was also assessed. Consequently, the amount of cesium ions adsorbed was in the following order: CB1000F < RB < CB200F < CB800F < CB600F < CB400F. Additionally, the solid–liquid separation ability of the prepared adsorbent after adsorption was evaluated. The results showed that CB400F, CB600F, and CB800F could be easily separated from the sample solution with the action of the magnetic field under our experimental conditions. Moreover, the effect of parameters, including contact time, adsorption temperature, and pH, on the adsorption of cesium ions was studied. The adsorption of cesium ions was rapid, and the equilibrium was reached within 10 min for CB400F. The adsorption capacity decreased with increasing adsorption temperatures (45 °C < 25 °C < 7 °C), and the optimal pH for removing cesium ions was approximately 10. Finally, the selectivity of cesium ion adsorption using CB400F was assessed; anions including chloride ions, sulfate ions, and nitrate ions did not interfere with the adsorption of cesium ions by CB400F. These results provide valuable information regarding the adsorption of cesium ions using the CB400F from aqueous media. The suggested treatment in this study significantly contributes to the development of recycling technology for biomass waste and/or purification of wastewater containing cesium ions.

Received 26th March 2024
Accepted 25th April 2024

DOI: 10.1039/d4su00149d

rsc.li/rscsus

Sustainability spotlight

In 2015, all member states of the United Nations embraced the sustainable development goals as a component of the 2030 agenda for sustainable development. This signifies that diverse initiatives have been implemented to establish a comprehensive 15 year strategy to attain these objectives. Particularly, goal 6 and goal 12 aim to develop efficient recycling technologies for establishing a sustainable society and reducing waste globally. Therefore, we focused on both the recycling technology of waste biomass bamboo (raw bamboo, RB) and wastewater purification to prevent clogging in adsorption treatment with adsorbent to establish a sustainable society and reduce global waste.

1 Introduction

In Japan, the Fukushima Daiichi Nuclear Power Plant accident occurred in 2011 and it led to widespread radiation release. Thus, it aroused the attention of many researchers towards finding a swift and sustainable technology for the decontamination of the radioactivity in the surrounding environment.[1–3] The accident was one of the worst nuclear accidents in nuclear history due to the release of certain nuclides, notably cesium, such as ^{137}Cs and ^{134}Cs, into the water environment. The ^{137}Cs level in Japan was approximately 1–2 $\times$ 10^{-3} Bq L^{-1} before 2011.[4] However, after 2011 in Japan, the levels of ^{137}Cs and ^{134}Cs increased to approximately 1.5 $\times$ 10^{13} Bq L^{-1} and approximately 1.8 $\times$ 10^{13} Bq L^{-1}.[5] These isotopes are beta and gamma emission nuclides with a half-life of approximately 2 and 30 years, respectively. Cesium nuclides have the potential to enter and accumulate within the human body through the consumption of contaminated food and/or drinking water.[6–9] Consequently, these can contribute to the development of various diseases

[a]*Faculty of Pharmacy, Kindai University, 3-4-1 Kowakae, Higashi-Osaka, Osaka, 577-8502, Japan. E-mail: kawasaki@phar.kindai.ac.jp*

[b]*Faculty of Pharmacy, Chiang Mai University, Suthep Road, Muang District, Chiang Mai, 50200, Thailand*

[c]*Center of Excellence for Innovation in Analytical Science and Technology for Biodiversity-based Economic and Society (I-ANALY-S-T_B.BES-CMU), Chiang Mai University, Chiang Mai, 50200, Thailand*

[d]*Faculty of Pharmaceutical Sciences, Nihon Pharmaceutical University, 10281 Komuro, Ina-machi, Kitaadachi-gun, Saitama, 362-0806, Japan*

[e]*Antiaging Center, Kindai University, 3-4-1 Kowakae, Higashi-Osaka, Osaka, 577-8502, Japan*

including thyroid cancer.[10] In addition, cesium nuclides can crush the biological cells of many organs and affect severe genetic disorders.[11–13] The release of cesium nuclides into the water environment also resulted in soil contamination and restricted the advancement of agriculture and animal tillage.[14–18] Therefore, according to the regulations of the International Atomic Energy Agency, low-rate radioactive wastewaters are defined as solutions with total radioactivity below 4.0×10^6 Bq L^{-1}.[19]

Various treatments have been proposed to prevent the spread of radionuclides in the biosphere, especially in water environments, such as membrane separation, evaporation, adsorption, reverse osmosis, ion exchange, precipitation, and filtration.[19] Among these treatments, adsorption is an easy, inexpensive, and more effective method, which is generally selected to adsorb radioactive waste from water environments.[20–23]

Furthermore, in 2015, all member states of the United Nations embraced the sustainable development goals as a component of the 2030 agenda for sustainable development. This signifies that diverse initiatives have been implemented to establish a comprehensive 15 year strategy to attain these objectives. Particularly, Goal 6 (clean water and sanitation) and Goal 12 (responsible consumption and production) aim to develop efficient recycling technologies for establishing a sustainable society and reducing waste globally.[24] One of these technologies changes waste biomass into valuable material, such as an adsorbent. In previous literature, activated charcoal, including various modified activated carbons, was prepared from waste biomass, and its characteristics and adsorption capability of cesium ions from the aqueous phase were evaluated.[25–28]

Bamboo is abundant in nature and is a renewable waste biomass, mostly found in Southeast Asian countries, including Thailand. A previous study reported that the physicochemical treatment of bamboo materials can enhance the adsorption capability of the adsorbate.[29,30] Additionally, the calcination of bamboo has gained attention as an adsorbent due to its enrichment with a microporous structure and higher surface area.[31] In a separate study, another researcher reported a simple separation method toward the use of magnetically activated carbon for preventing clogging in the water purification process.[32,33] Therefore, we focused on both the recycling technology of waste biomass bamboo (raw bamboo, RB) and wastewater purification to prevent clogging during the adsorption treatment with the adsorbent to establish a sustainable society and reduce global waste.

Based on the current understanding, there is a lack of research on the utilization of magnetically-activated charcoal derived from waste biomass bamboo as an adsorbent for removing cesium ions, despite its significant potential. Therefore, the magnetically activated charcoal was prepared from RB, and its characteristics including pH_{pzc}, specific surface area, and surface functional groups were investigated. Additionally, the adsorption capability of cesium ions from aqueous solution under several experimental conditions such as contact time, adsorption temperature, solution pH, and the effect of coexistences using the prepared adsorbent was also addressed in detail. Finally, the obtained results in this study contribute to the development of recycling technology for biomass waste and/or purification of wastewater containing cesium ions.

2 Experimental section

2.1 Materials

RB was obtained from Thailand. Cesium standard solution (CsCl in water), hydrochloric acid (HCl), sodium hydroxide (NaOH), and iron(III) nitrate nonahydrate ($Fe(NO_3)_3 \cdot 9H_2O$) were supplied from FUJIFILM Wako Pure Chemical Co., Ltd (Japan). Potassium chloride, sodium chloride, sodium sulfate, and sodium nitrate were also purchased from FUJIFILM Wako Pure Chemical Ind., Ltd (Special grade reagent, Japan).

Calcined bamboo treated with iron(III) nitrate nonahydrate at different temperatures was prepared using the following method: RB and iron(III) nitrate nonahydrate were mixed at an RB/$Fe(NO_3)_3 \cdot 9H_2O$ mass ratio of 1 : 1.5 in a crucible. Then, the mixtures were calcined at 200 °C, 400 °C, 600 °C, 800 °C, or 1000 °C for 2 h by KDF S-80 instrument (Denken-Highdental Co., Ltd, Japan) and the calcination temperature was held for 2 h, and then, the obtained materials were naturally cooled in this study; the samples were labeled as CB200F, CB400F, CB600F, CB800F, and CB1000F, respectively.

2.2 Characteristics of raw bamboo (RB) and prepared samples

The physical and chemical characteristics of both RB and the prepared samples were evaluated using the following methods: Scanning Electron Microscope (SEM) images were acquired using an SU1510 instrument from Hitachi High-Technologies Co., Ltd, Japan. Fourier-transform infrared (FT-IR) spectroscopy was also measured using an FT-IR-460Plus spectrometer (JASCO, Co., Japan). The specific surface area was determined using a NOVA4200*e* instrument (Yuasa Ionics, Japan). The point of zero charge (pH_{pzc}) and surface functional groups, including acidic or basic functional groups, were also determined following the methods as detailed in prior studies by Faria *et al.*[34,35] and Boehm's titration method,[36,37] respectively. Finally, X-ray diffraction (XRD) patterns of CB400F and Fe_3O_4 were measured using a MiniFlex II instrument (Rigaku, Japan).

2.3 Adsorption capacity of cesium ions

In this study, an initial screening experiment was carried out to evaluate the adsorption capacity of cesium ions using RB and prepared samples. Cesium ion solution (50 mg L^{-1}, 50 mL) and each adsorbent (0.05 g) were mixed and reacted at 100 rpm for 24 h at 25 °C. After the completion of the reaction, the solution was filtered through a 0.45 μm membrane filter. The equilibrium concentration of cesium ions was subsequently quantified using an inductively coupled plasma optical emission spectrometer (iCAP-7600 Duo, Thermo Fisher Scientific Inc., Japan). Finally, the quantity of cesium ions adsorbed was calculated by the differences between initial and equilibrium concentrations.

2.4 Changes in the adsorption capacity of cesium ions under several experimental conditions

The assessment of adsorption isotherms was conducted as follows: cesium ions solutions at different concentrations (10 mg L^{-1}, 20 mg L^{-1}, 30 mg L^{-1}, 40 mg L^{-1}, or 50 mg L^{-1}, 50 mL) were mixed with 0.05 g of CB400F and then reacted at 100 rpm for 24 h at 7 °C, 25 °C, and 45 °C. For analyzing adsorption isotherm models, typically, Langmuir (eqn (1)) and Freundlich (eqn (2)) isotherms were chosen.[38,39] The following equation presents the linearized expression of Langmuir's isotherm model:

$$1/q = 1/(q_{max}K_LC_e) + 1/q_{max} \quad (1)$$

where q is the quantity of cesium ions adsorbed (mg g^{-1}), q_{max} is the maximum quantity adsorbed (mg g^{-1}), C_e is the equilibrium concentration (mg L^{-1}), and K_L is the Langmuir isotherm constant (binding energy) (L mg^{-1}).

Moreover, the linear form of Freundlich's isotherm model is:

$$\log q = \log C_e + \log K_F \quad (2)$$

where K_F and $1/n$ are the adsorption capacity and strength of adsorption, respectively.

Next, the effect of contact time on the adsorption of cesium ions was measured; cesium ion solution at 50 mg L^{-1} (50 mL) and CB400F of 0.05 g was mixed and reacted at 100 rpm for 10 min, 1 h, 6 h, 9 h, 15 h, 18 h, 21 h, and 24 h at 25 °C. Adsorption kinetics were assessed by the pseudo-first-order (PFOM, eqn (3)) and pseudo-second-order kinetic models (PSOM, eqn (4)).[40,41]

$$\ln(q_e - q_t) = \ln q_e - k_1 t \quad (3)$$

$$\frac{t}{q_t} = \frac{t}{q_e} + \frac{1}{k_2 \times q_e^2} \quad (4)$$

where q_e (mg g^{-1}) is the quantity of the adsorbed cesium ions at equilibrium, q_t (mg g^{-1}) is the quantity of cesium ions adsorbed at time t, k_1 (h^{-1}) is the overall constant in the pseudo-first-order model, and k_2 (g mg^{-1} h^{-1}) is the pseudo-second-order adsorption constant.

Finally, 50 mg L^{-1} cesium ion solution at different pH (pH 2, 4, 6, 8, 10, or 12 and 50 mL) and CB400F of 0.05 g was mixed and reacted at 100 rpm for 24 h at 25 °C. The quantity of the adsorbed cesium ions was calculated using the method described in Section 2.3. Moreover, electron probe microanalysis was performed both before and after the adsorption of cesium ions using a JXA-8530F microanalyzer (JEOL, Japan).

2.5 Effect of coexistences on the adsorption characteristics of cesium ions

In order to investigate the adsorption selectivity of cesium ions in an aqueous phase, a complex solution system (50 mL) was prepared by adding 0.05 g of CB400F. Potassium (potassium chloride) and sodium (sodium chloride) ions were used as the interfering cations. Meanwhile, chloride (sodium chloride), sulfate (sodium sulfate), and nitrate (sodium nitrate) ions were used as anions in this study. The initial concentration of each anion and cations was set at 50 mg L^{-1}. The binary solution systems (cesium ion + cation or anion) were shaken for 24 h at 100 rpm and 25 °C. After the adsorption, the sample solution underwent separation through a 0.45 μm membrane filter. The concentration of each cation was measured using the iCAP-7600 Duo instrument, while the concentration of each anion was measured using a DIONEX ICS-900 (Thermo Fisher Scientific Inc., Tokyo, Japan) following the previously reported experimental conditions.[42]

2.6 Recycling performance of CB400F for removal of cesium ions

To elucidate the recycling performance of CB400F, the adsorption/desorption capability of cesium ions was demonstrated. First, 100 mg L^{-1} cesium ion solution (50 mL) and CB400F of 0.1 g were mixed and reacted at 100 rpm for 24 h at 25 °C. The quantity of cesium ions adsorbed was also calculated using the method described in Section 2.3. After adsorption, CB400F was collected, dried at 50 °C, and used for desorption experiments. The desorption experiments were performed according to the following methods. Collected CB400F (0.05 g) was mixed with a desorption solution such as distilled water, 1 mmol L^{-1} sodium hydroxide solution, or 1 mmol L^{-1} hydrochloric acid solution (50 mL). The reaction solution was shaken at 100 rpm for 24 h at 25 °C. After desorption, the solution was then filtered through a 0.45 μm membrane filter. Subsequently, the concentration of cesium ions was measured using the iCAP-7600 Duo instrument. The desorption capacity was calculated using the equilibrium concentrations.

3 Results and discussion

3.1 Characteristics of RB and magnetic carbonaceous material (CB) adsorbents

The SEM images of RB and the prepared CB samples are presented in Fig. 1. The RB surface exhibited a dense and constricted morphology; compared to CB samples, the number of pores on the CB surface increased with increasing calcination temperatures. In particular, the CB400F, CB600F, and CB800F models were composed of porous material with a rougher surface and looser structure. Furthermore, in Fig. 2, the FT-IR spectra of the prepared samples are presented. Some CB samples showed a broad and intense band within the range of 3200–3600 cm^{-1} due to the presence of free and hydrogen-bonded OH stretching vibrations. Additionally, a prominent peak in the spectral range of 1500–1700 cm^{-1} was observed, indicating the presence of C–O carbonyl stretching vibrations. In Table 1, the pH_{pzc}, specific surface area, and the amount of acid or basic functional groups of CB samples are presented. The value of pH_{pzc} increased from 5.4 to 9.7 with increasing calcination temperatures, and a similar trend was observed in the value of specific surface area. Furthermore, the values of CB400F, CB600F, and CB800F were greater than those of other samples. Finally, the amount of acid or basic functional groups of RB was 0 or 0.81 mmol g^{-1}, respectively, and the amount of basic functional groups decreased with increasing calcination

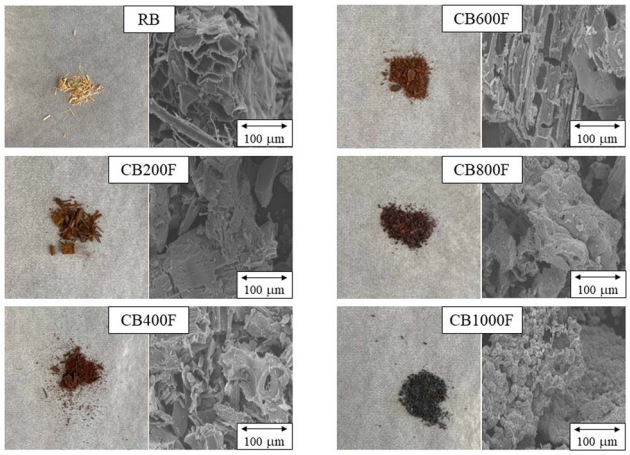

Fig. 1 SEM images of the prepared samples.

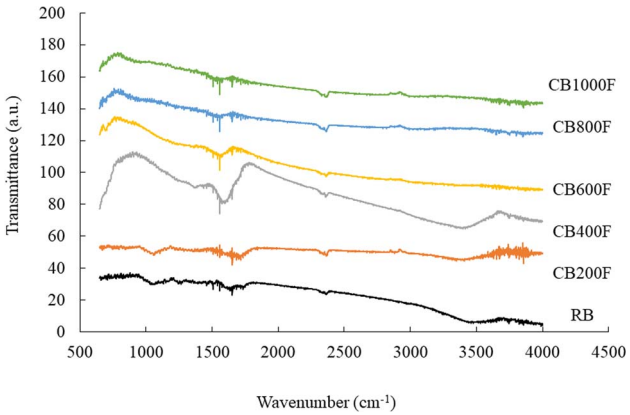

Fig. 2 FT-IR spectra of the prepared samples.

temperatures. These changes were consistent with the results of FT-IRs.

3.2 Amount of cesium ions adsorbed using RB and CB samples

Fig. 3 shows the adsorption capacity of cesium ions. Under our experimental conditions, the amount adsorbed followed this order: CB1000F (0.08 mg g^{-1}) exhibited the lowest adsorption, followed by RB (0.1 mg g^{-1}), CB200F (0.4 mg g^{-1}), CB800F (0.8 mg g^{-1}), CB600F (10.1 mg g^{-1}), and CB400F (12.8 mg g^{-1}). The characteristics of both RB and CB samples suggest that the specific surface area plays a significant role in enhancing the adsorption capacity of cesium ions in the aqueous phase. Nevertheless, additional research is imperative to comprehensively understand the adsorption mechanism of cesium ions when employing these prepared samples. Recently, some studies have focused on a separation method toward the use of magnetic carbon for preventing clogging during the water purification process.[32,33] Thus, the efficiency of solid–liquid separation using CB samples was evaluated in this study. Fig. 4 shows the effective separation of CB400F, CB600F, and CB800F from the sample solution due to the action of the magnetic field, suggesting the potential utility of prepared CB samples in water purification for solid–liquid separation. In addition, the existence of Fe_3O_4 in CB400F was measured by XRD patterns (Fig. 5). As a result, the peaks of Fe_3O_4 were clearly detected in CB400F. Therefore, CB400F showed the efficiency of solid–liquid separation under our experimental conditions. These data support the abovementioned results and discussion.

3.3 Effect of contact time on the adsorption of cesium ions using CB400F

The time course for the adsorption of cesium ions is shown in Fig. 6, it indicates a rapid adsorption rate with equilibrium achieved within 10 min for CB400F. This rapid cesium ion adsorption can be explained by the availability of active sites on the adsorbent surface, which indicates that rapid initial adsorption (within 9 h) was likely due to the outer surface binding, while slower adsorption (after 9 h) was likely due to inner surface binding.[43,44]

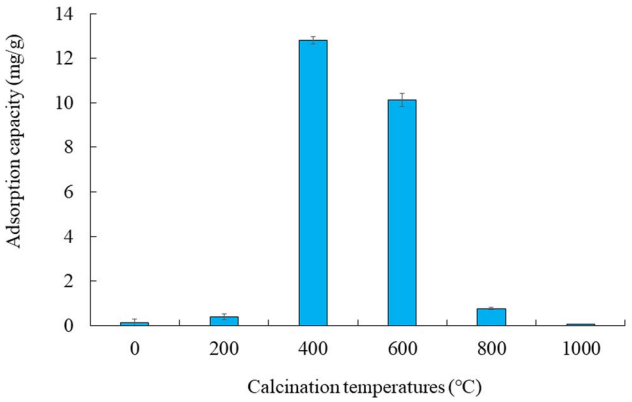

Fig. 3 Adsorption capacity of cesium ions. Initial concentration: 50 mg L^{-1}, sample volume: 50 mL, adsorbent: 0.05 g, temperature: 25 °C, contact time: 24 h, 100 rpm.

Table 1 Characteristics of the prepared samples

Samples	RB	CB200F	CB400F	CB600F	CB800F	CB1000F
pH_{pzc}	5.4	5.1	7.8	8.8	9.9	9.7
Specific surface area (m^2 g^{-1})	3.3	14.0	50.6	50.5	56.9	24.1
Amount of acid functional groups (mmol g^{-1})	0	0	0.10	0.07	0.13	0.02
Amount of basic functional groups (mmol g^{-1})	0.81	0.87	0.83	0.08	0.11	0

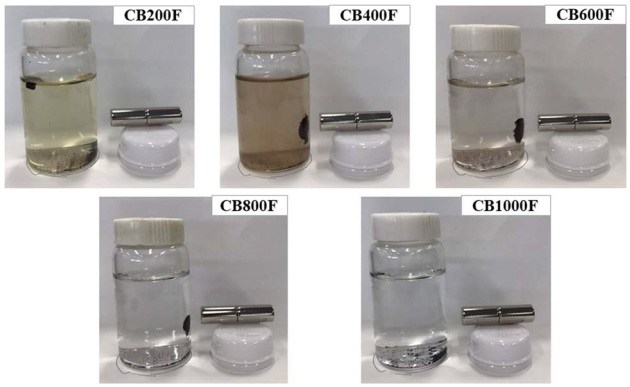

Fig. 4 Photographs of sample solutions after adsorption.

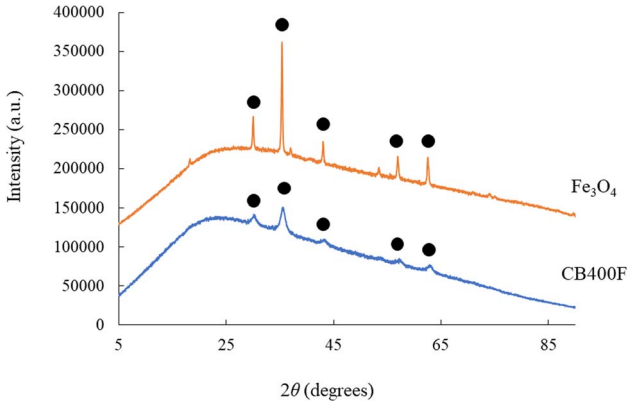

Fig. 5 XRD patterns of CB400F and Fe_3O_4.

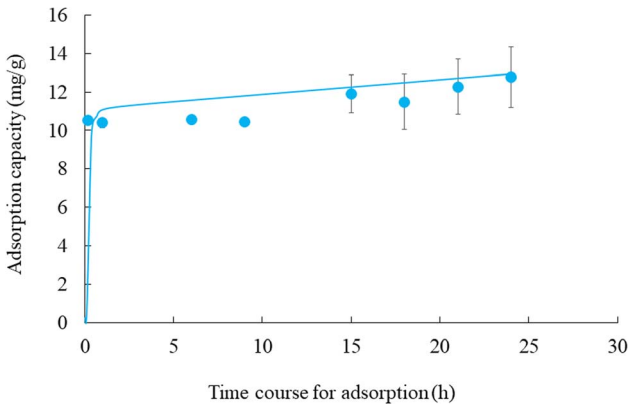

Fig. 6 Time course of adsorption of cesium ions. Initial concentration: 50 mg L^{-1}, sample volume: 50 mL, adsorbent: 0.05 g, temperature: 25 °C, contact time: 10 min, 1 h, 6 h, 9 h, 15 h, 18 h, 21 h, and 24 h, 100 rpm.

Additionally, PFOM and PSOM were used to comprehend the adsorption mechanism of cesium ions. Among the two applied kinetic models, the PFOM model appears unsuitable for describing the adsorption of cesium ions with CB400F (Table 2). According to this model, the correlation coefficient was not high (0.752), and the theoretical value of adsorption at equilibrium (12.8 mg g^{-1}) is significantly different from the experimental value (2.8 mg g^{-1}). In contrast, under our experimental conditions, the PSOM exhibits a higher correlation coefficient of 0.992. Additionally, the adsorption capacity of cesium ions obtained from this kinetic model is closely aligned with the experimental value (12.6 mg g^{-1}). Therefore, these results indicate that the pseudo-second-order adsorption mechanism could explain the adsorption of cesium ions by CB400F.

3.4 Effect of initial concentration and temperature on the adsorption of cesium ions using CB400F

Fig. 7 shows the adsorption isotherms of cesium ions at different temperatures. The amount adsorbed increased with decreasing adsorption temperatures (45 °C < 25 °C < 7 °C). These results demonstrate that the adsorption process of cesium ions is exothermic. The adsorption isotherms parameters are presented in Table 3; the data clearly show that the Langmuir model (correlation coefficient: 0.906 to 0.929) is more appropriate than the Freundlich model (correlation coefficient: 0.752 to 0.939) for the adsorption of cesium ions. Moreover, the Langmuir adsorption isotherm proves to be a valuable tool for calculating the maximum quantity of cesium ion adsorption. The maximum amount quantity (q_{mas}) increased with decreasing adsorption temperatures [45 °C (11.0 mg g^{-1}) < 7 °C (20.7 mg g^{-1})]; these phenomena showed similar trends in the adsorption isotherms (Fig. 6). Finally, cesium ions were easily adsorbed onto the CB400F surface when $1/n$ was in the 0.1–0.5 range.[45] Conversely, when $1/n$ was >2, cesium ions did not easily adsorb onto the surface of CB400F. In this study, the value of $1/n$ was 0.4–0.8, indicating that cesium ions were easily adsorbed onto CB400F under our experimental conditions.

To further confirm the adsorption of cesium ions onto CB400F surface, the elemental distribution of cesium (Cs) onto CB400F before and after the adsorption was evaluated (Fig. 8). Based on the results, the amount of cesium (Cs) increased after the adsorption treatment. This indicates that cesium ions were adsorbed onto the CB400F surface and supports the adsorption phenomenon mentioned above in this experiment.

Finally, many studies have successfully been able to remove cesium ions from the aqueous phase using various types of biomass adsorbents,[46–51] and these were compared with this study (Table 4). This demonstrated that CB400F exhibited superior performance in removing cesium ions from the aqueous phase (except for nitric acid-modified bamboo charcoal and Mucilaginous seeds of *Ocimum basulicum*).

3.5 Effect of pH on the adsorption of cesium ions using CB400F

Fig. 9 shows the adsorption capacity of cesium ions at different pH conditions. The study found that higher cesium ion adsorption was achieved at pH 10 compared to other pH conditions, and adsorption was seriously interrupted at lower pH (<4). There are two underlying reasons contributing to this phenomenon: the competition of H_3O^+ with cesium ions, as well as the electrostatic repulsion between cesium ions and the positively charged surface of CB400F (the value of pH_{pzc} is 7.8). Similar adsorption

Table 2 Fitting results of kinetic data using PFOM and PSOM

		Pseudo-first-order model			Pseudo-second-order model		
Sample	$q_{e,exp}$ (mg g^{-1})	K_1 (h^{-1})	$q_{e,cal}$ (mg g^{-1})	R^2	K_2 (mg g^{-1} h^{-1})	$q_{e,cal}$ (mg g^{-1})	R^2
CB400F	12.8	0.07	2.8	0.752	0.08	12.6	0.992

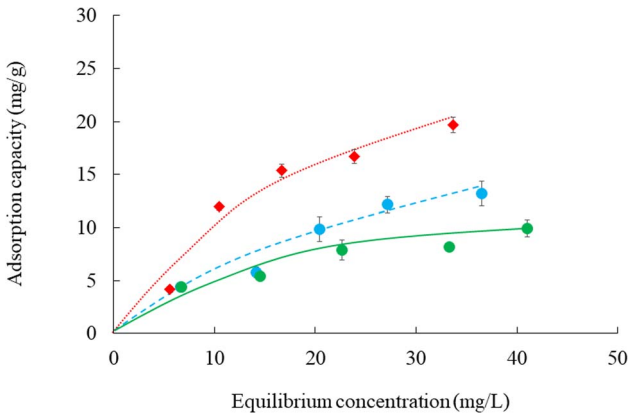

Fig. 7 Adsorption isotherms of cesium ions at different temperatures. Initial concentration: 10–50 mg L^{-1}, sample volume: 50 mL, adsorbent: 0.05 g, temperature: 7 (♦), 25 (●), and 45 (●) °C, contact time: 24 h, 100 rpm.

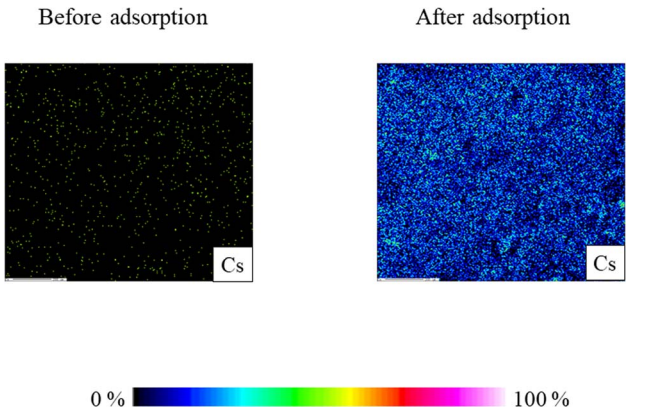

Fig. 8 Elemental distributions of cesium (Cs) before and after adsorption. Initial concentration: 50 mg L^{-1}, sample volume: 50 mL, adsorbent: 0.05 g, temperature: 25 °C, contact time: 24 h, 100 rpm.

mechanisms have already been reported in previous studies.[52,53] Conversely, it is assumed that under basic conditions, the adsorption of cesium ions was also significantly influenced under an alkaline state (>10), possibly due to the formation of cesium hydroxide. Furthermore, the presence of negative ions in cesium hydroxide ($Cs(OH)_2^-$) might increase an electrostatic repulsion among hydroxide ions or the negatively charged surface of CB400F, inhibiting cesium ion adsorption.[53,54]

3.6 Effect of coexistences on the adsorption of cesium ions

Fig. 10 shows the effect of coexistence on the adsorption of cesium ions. The amount of adsorbed cesium ions onto CB400F in a single solution system was 12.8 mg g^{-1}, while the amount adsorbed in a cation complex solution system clearly decreased. Furthermore, the amount of cesium ions adsorbed in an anion complex solution system was significantly unchanged compared to the single solution system. These phenomena indicate that anions, including chloride ions, sulfate ions, and nitrate ions, have a limited impact on the adsorption capacity of cesium ions using CB400F. Consequently, CB400F exhibits potential utility as an effective adsorbent for the removal of cesium ions from aqueous solutions.

3.7 Cesium ions adsorption/desorption capacity of CB400F

CB400F's capacity for desorption of the adsorbed cesium ions was assessed using various desorption solutions such as distilled water, 1 mmol L^{-1} sodium hydroxide solution, or 1 mmol L^{-1} hydrochloric acid solution. The desorption percentages of cesium ions from CB400F using distilled water, 1 mmol L^{-1} sodium hydroxide solution, or 1 mmol L^{-1} hydrochloric acid solution were 0%, 48.5%, or 0%, respectively. The optimal pH condition for the removal of cesium ions was approximately 10 in Section 3.5. Therefore, adsorbed cesium ions were easily desorbed under acidic conditions. The results show that hydrochloric acid solution is the suitable solution for the desorption of cesium ions from CB400F under the explored experimental conditions.

3.8 Adsorption mechanism of cesium ions using CB400F

Previous studies have reported the adsorption mechanism between an adsorbent and heavy metal in detail.[55,56] Therefore,

Table 3 Fitting results of isotherm data using Freundlich and Langmuir models

		Langmuir isotherm model			Freundlich isotherm model		
Sample	Temperature (°C)	K_L (L mg^{-1})	q_{max} (mg g^{-1})	R^2	log K_F	$1/n$	R^2
CB400F	5	5.3	20.7	0.929	0.1	0.8	0.870
	25	26.6	21.1	0.906	0.03	0.7	0.939
	45	10.8	11.0	0.908	0.3	0.4	0.752

Table 4 Comparison of the adsorption capacity of cesium ions with other reported adsorbents

Adsorbents	Adsorption capability (mg g^{-1})	pH	Temperature (°C)	Initial concentration (mg L^{-1})	Contact time (h)	Adsorbent (g L^{-1})	References
Coal and chitosan	3.0	—	Ambient	3.9	24	5–10	46
Coconut shell-activated carbon	0.76	7.3–10.0	—	10–30	24	0.67–3.3	47
Bamboo charcoal	0.17	4.0	20	100	6	1.0	48
Nitric acid-modified bamboo charcoal	45.87	4.0	20	100	6	1.0	48
Brewery's waste biomass	10.1	4.0	30	1064	3	2	49
Pre-treated arca shell biomass	3.93	1–7	20 ± 2	10–500	0.17–7	0.1–15.0	50
Mucilaginous seeds of *Ocimum basulicum*	160	—	28	10 000	2	25	51
CB400F	12.8	—	25	50	24	1.0	This study

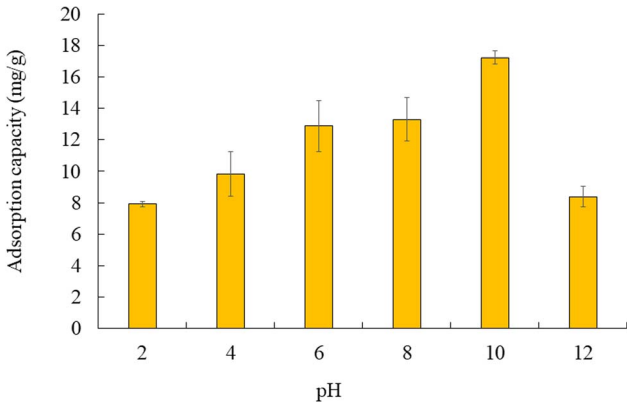

Fig. 9 Adsorption capacity of cesium ions at different pH conditions. Initial concentration: 50 mg L^{-1}, sample volume: 50 mL, adsorbent: 0.05 g, temperature: 25 °C, contact time: 24 h, 100 rpm.

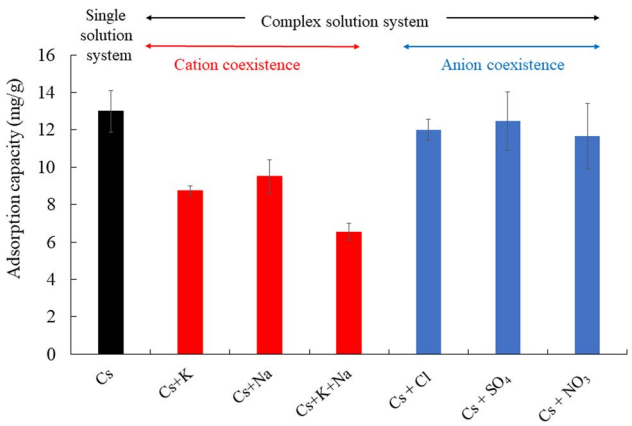

Fig. 10 Effect of coexistence on the adsorption of cesium ions. Initial concentration: 50 mg L^{-1}, sample volume: 50 mL, adsorbent: 0.05 g, temperature: 25 °C, contact time: 24 h, 100 rpm.

we briefly summarized the schematic mechanism of cesium ions adsorption using CB400F (Fig. 11). The adsorption mechanisms can mainly be divided into two processes in this study. One is cesium ions are adsorbed by the CB400F surface due to the surface area and/or surface charge (physisorption). Another is electrostatic attraction occurring between the surface

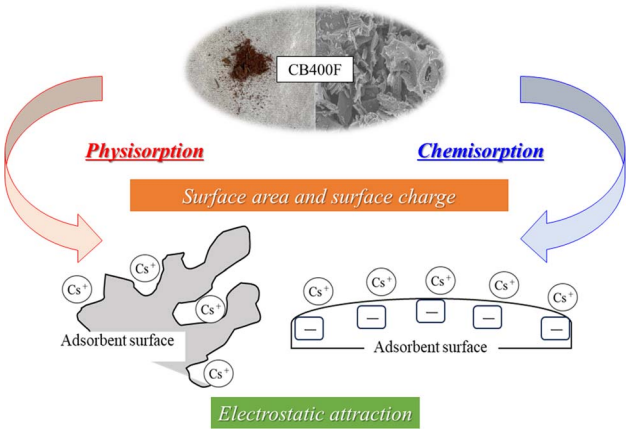

Fig. 11 The schematic mechanism of cesium ions adsorption using CB400F.

functional groups and cesium ions (chemisorption). However, further studies are necessary to elucidate the adsorption mechanism of cesium ions in detail using CB400F.

4. Conclusions

In this study, magnetic carbonaceous materials derived from waste bamboo were prepared, and the findings demonstrate that the adsorption capability of cesium ions using CB400F (12.8 mg g^{-1}) was higher compared to other prepared adsorbents (0.08–10.1 mg g^{-1}). Additionally, CB400 exhibited superior performance in achieving solid–liquid separation during water purification. The optimization of the factors, including contact time (within 10 min), temperature (45 °C < 25 °C < 7 °C), and pH (approximately 10), on cesium ion adsorption using CB400 was determined. In addition, the adsorption process followed the pseudo-second-order model (correlation coefficient: 0.992). The experimental adsorption data are well-fitted by the Langmuir model (correlation coefficient: 0.906–0.929) compared to the Freundlich model (correlation coefficient: 0.752–0.939). To confirm the adsorption of cesium ions onto the CB400F surface, the elemental distribution of Cs onto the CB400 surface was evaluated before and after the adsorption treatment. The intensity of Cs was observed to exhibit an

increase following the adsorption process in comparison to its initial state. Finally, anions, including chloride ions, sulfate ions, and nitrate ions, exhibited limited influence on the adsorption capacity of cesium ions using CB400F. Consequently, CB400F demonstrates promise as a valuable adsorbent for the removal of cesium ions from aqueous solutions.

Author contributions

Fumihiko Ogata: conceptualization, project administration, writing–original draft, and writing–review and editing; Noriaki Nagai: investigation and visualization; Taiki Ogawa: investigation and visualization; Yugo Uematsu: investigation and visualization; Chalermpong Saenjum: investigation and visualization; Shigeharu Tanei: methodology; Naohito Kawasaki; project administration, supervision, and writing–review and editing.

Conflicts of interest

There are no conflicts to declare.

Acknowledgements

This work is supported by JSPS KAKENHI (JP22K06674).

References

1 M. R. Awual, Ring size dependent crown ether based mesoporous adsorbent for high cesium adsorption from wastewater, *Chem. Eng. J.*, 2016, **303**, 539–546.
2 M. R. Awual, M. Miyazaki, T. Taguchi, H. Shiwaku and T. Yaita, Encapsulation of cesium from contaminated water with highly selective facial organic-inorganic mesoporous hybrid adsorbent, *Chem. Eng. J.*, 2016, **291**, 128–137.
3 M. R. Awual, T. Yaita, M. Miyazaki, D. Matsumura, H. Shiwaku and T. Taguchi, A reliable hybrid adsorbent for efficient radioactive cesium accumulation from contaminated wastewater, *Sci. Rep.*, 2016, **6**, 19937.
4 M. Aoyama and K. Hirose, Artificial radionuclides database in the Pacific Ocean: HAM database, *Sci. World J.*, 2004, **4**, 200–215.
5 D. Parajuli, H. Tanaka, Y. Hakuta, K. Minami, S. Fukuda, K. Umeoka, R. Kamimura, Y. Hayashi, M. Ouchi and T. Kawamoto, Dealing with the aftermath of Fukushima Daiichi nuclear accident: Decontamination of radioactive cesium enriched ash, *Environ. Sci. Technol.*, 2013, **47**, 3800–3806.
6 M. R. Awual, T. Yaita, T. Taguchi, H. Shiwaku, S. Suzuki and Y. Okamoto, Selective cesium removal from radioactive liquid waste by crown ether immobilized new class conjugate adsorbent, *J. Hazard. Mater.*, 2014, **278**, 227–235.
7 T. J. Yasunari, A. Stohl, R. S. Hayano, J. F. Burkhart, S. Eckhardt and T. Yasunari, Cesium-137 deposition and contamination of Japanese soils due to the Fukushima nuclear accident, *Proc. Natl. Acad. Sci. U. S. A.*, 2011, **108**, 19530–19534.
8 R. Chen, H. Tanaka, T. Kawamoto, M. Asai, C. Fukushima, M. Kurihara, M. Ishizaki, M. Watanabe, M. Arisaka and T. Nankawa, Thermodynamics and mechanism studies on electrochemical removal of cesium ions from aqueous solution using a nanoparticle film of copper hexacyanoferrate, *ACS Appl. Mater. Interfaces*, 2013, **24**, 12984–12990.
9 H. Long, P. Wu, L. Yang, Z. Huang, N. Zhu and Z. Hu, Efficient removal of cesium from aqueous solution with vermiculite of enhanced adsorption property through surface modification by ethylamine, *J. Colloid Interface Sci.*, 2014, **428**, 295–301.
10 H. Yang, H. Yu, J. Sun, J. Liu, J. Xia, J. Fang, Y. Li, F. Qu, A. Song and T. Wu, Facile synthesis of mesoporous magnetic AMP polyhedric composites for rapid and highly efficient separation of Cs^+ from water, *Chem. Eng. J.*, 2017, **317**, 533–543.
11 V. J. Sharavanan, M. Sivaramakrishnan, N. Sivarajasekar, N. Senthilrani, R. Kothandan, N. Dhakal, S. Sivamani, P. L. Show, M. R. Awual and M. Naushad, Pollutants inducing epigenetic changes and diseases, *Environ. Chem. Lett.*, 2020, **18**, 325–343.
12 H. Yang, H. Li, J. Zhai, L. Sun, Y. Zhao and H. Yu, Magnetic prussian blue/graphene oxide nanocomposites caged in calcium alginate microbeads for elimination of cesium ions from water and soil, *Chem. Eng. J.*, 2014, **246**, 10–19.
13 B. Hu, B. Fugetsu, H. Yu and Y. Abe, Prussian blue caged in spongiform adsorbents using diatomite and carbon nanotubes for elimination of cesium, *J. Hazard. Mater.*, 2012, **217–218**, 85–91.
14 C. W. Park, B. H. Kim, H. M. Yang, B. K. Seo, J. K. Moon and K. W. Lee, Removal of cesium ions from clays by cationic surfactant intercalation, *Chemosphere*, 2017, **168**, 1068–1074.
15 I. Lee, C. W. Park, S. S. Yoon and H. M. Yang, Facile synthesis of copper ferrocyanide-embedded magnetic hydrogel beads for the enhanced removal of cesium from water, *Chemosphere*, 2019, **224**, 776–785.
16 S. R. H. Vanderheyden, J. Yperman, R. Carleer and S. Schreurs, Enhanced cesium removal from real matrices by nickel-hexacyanoferrate modified activated carbons, *Chemosphere*, 2018, **202**, 569–575.
17 A. Zehad, G. J. Islam, M. Rashid, N. J. Juthy and S. Zannah, Antidiabetic and antihyperlipidemic activities of methanolic leaf extract of stephania japonica in alloxan induced diabetic rats, *Pharmacol. Pharm.*, 2017, **8**, 109–127.
18 S. Zannah, M. Asaduzzaman, A. A. A. Bari, Y. Ali, G. J. Islam, A. H. M. K. Khurshid Alam, H. Ali and M. Rashid, Antidiabetic drugs in combination with hydroxychloroquine improve glycemic control in alloxan induced diabetic rats, *Pharmacol. Pharm.*, 2014, **5**, 725–735.
19 B. Işık, A. E. Kurtoğlu, G. Gürdağ and G. Keçeli, Radioactive cesium ion removal from wastewater using polymer metal oxide composites, *J. Hazard. Mater.*, 2021, **403**, 123652.

20 A. S. Bhatt, D. K. Bhat and M. S. Santosh, Electrical and magnetic properties of chitosan-magnetite nanocomposites, *Phys. B*, 2010, **405**, 2078–2082.
21 N. A. Chapman and I. G. McKinley, *The Geological Disposal of Nuclear Waste*, Wiley-Interscience, New York, 1987, p. 49.
22 B. Li, H. Liu, X. Ye, S. Li and Z. Wu, Rubidium and cesium ion adsorption by a potassium titanium silicate-calcium alginate composite adsorbent, *Sep. Sci. Technol.*, 2014, **49**, 1076–1085.
23 Ş. Sert and M. Eral, Uranium adsorption studies on aminopropyl modified mesoporous sorbent (NH_2 – MCM – 41) using statistical design method, *J. Nucl. Mater.*, 2010, **406**, 285–292.
24 Y. Uematsu, F. Ogata, N. Nagai, S. Chalermpong, T. Nakamura and N. Kawasaki, In vitro removal of paraquat and diquat from aqueous media using raw and calcined basil seed, *Heliyon*, 2021, **7**, e07644.
25 S. R. H. Vanderheyden, R. Van Ammel, K. Sobiech-Mature, K. Vanerppelen, S. Schreurs, W. Schroeyers, J. Yperman and R. Carleer, Adsorption of cesium on different types of activated carbon, *J. Radioanal. Nucl. Chem.*, 2016, **310**, 301–310.
26 S. Khandarker, M. F. Chowdhury, Md. R. Awual, A. Islam and T. Kuba, Efficient cesium encapsulation from contaminated water by cellulosic biomass based activated wood charcoal, *Chemosphere*, 2021, **262**, 127801.
27 X. Liu, G. R. Chen, D. J. Lee, T. Kawamoto, H. Tanaka, M. L. Chen and Y. K. Luo, Adsorption removal of cesium from drinking waters: A mini review on use of biosorbents and other adsorbents, *Bioresour. Technol.*, 2014, **160**, 142–149.
28 S. R. H. Vanderheyden, J. Yperman, R. Carleer and S. Schreurs, Enhanced cesium removal from real matrices by nickel-hexacyanoferrate modified activated carbon, *Chemosphere*, 2018, **202**, 569–575.
29 S. Khandaker, Y. Toyohara, S. Kamida and T. Kuba, Adsorptive removal of secium from aqueous solution using oxidized bamboo charcoal, *Water Res. Ind.*, 2018, **19**, 35–46.
30 Y. Fan, B. Wang, S. Yuan, X. Wu, J. Chen and L. Wang, Adsorptive removal of chloramphenicol from wastewater by NaOH modified bamboo charcoal, *Bioresour. Technol.*, 2010, **101**, 7661–7664.
31 R. S. Zhao, J. P. Yuan, T. Jiang, J. B. Shi and C. G. Cheng, Application of bamboo charcoal as solid-phase extraction adsorbent for the determination of atrazine and simazine in environmental waster samples by high-performance liquid chromatography-ultraviolet detector?, *Talanta*, 2008, **76**, 956–959.
32 W. Jiang, L. Zhang, X. Guo, M. Yang, Y. Lu, Y. Wang, Y. Zheng and G. Wei, Adsorption of cationic dye from water using an iron oxide/activated carbon magnetic composites prepared from sugarcane bagasse by microwave method, *Environ. Technol.*, 2021, **42**, 337–350.
33 B. B. Joanna and J. K. Agata, Cesium ion sorption on hybrid pectin-Prussian blue beads: Bath and column studies to remove radioactive cesium from contaminated wastewater, *Hydrometallurgy*, 2022, **213**, 105937.
34 P. C. C. Faria, J. J. M. Orfao and M. F. R. Pereira, Adsorption of anionic and cationic dyes on activated carbons with different surface chemistries, *Water Res.*, 2004, **38**, 2043–2052.
35 G. Lee, C. Chen, S. T. Yang and W. S. Ahn, Enhanced adsorptive removal of fluoride using mesoporous alumina, *Microporous Mesoporous Mater.*, 2010, **127**, 152–156.
36 H. P. Boehm, Chemical identification of surface groups, *Adv. Catal.*, 1996, **16**, 179–274.
37 H. P. Boehm, Functional groups on the surfaces of solids, *Angew. Chem., Int. Ed. Engl.*, 1996, **5**, 533–544.
38 I. Langmuir, The adsorption of gases on plane surfaces of glass, mica and platinum, *J. Am. Chem. Soc.*, 1918, **40**, 1361–1403.
39 H. Freundlich, Over the adsorption in solution, *J. Phys. Chem.*, 1906, **57**, 384–471.
40 D. Karamanis and P. A. Assimakopoulos, Efficiency of aluminum-pillared montmorillonite on the removal cesium and copper from aqueous solutions, *Water Res.*, 2007, **41**, 1897–1906.
41 Y. S. Ho and G. MacKay, Pseudo-second-order model for sorption process, *Process Biochem.*, 1999, **34**, 451–465.
42 F. Ogata, S. Kawamoto, A. Tabuchi, M. Toda, M. Otani and N. Kawasaki, Feasibility of nickel-aluminum complex hydroxides for recovering tungsten ions from aqueous media, *Sustainability*, 2022, **14**, 3219.
43 G. A. Rahman Dakroury, S. F. Abo-Zahra, H. S. Hassan and H. E. Ahmed Ali, Improvement of the sorption behavior of aluminum silicate composite toward ^{134}Cs and ^{60}Co radionuclides by non-living biomass of Chlorella vulgaris, *Environ. Sci. Pollut. Res.*, 2020, **27**, 21109–21125.
44 *Proceedings of 1989 SME Symposium on Biotechnology in Minerals and Metal Processing*, ed. M. R. Ferguson, T. M. Peterson, A. Jeffers, B. J. Scheiver, F. M. Doyle, and S. K. Kawatra, SME, 1989, vol. 24, pp. 201–207.
45 I. Abe, M. Hayashi and M. Kitagawa, Studies on the adsorption of surfactants on activated carbon, *J. Jpn. Oil Chem. Soc.*, 1976, **25**, 145–150.
46 J. Mizera, G. Mizerová, V. Machovič and L. Borecká, Sorption of cesium, cobalt and europium on low-rank coal and chitosan, *Water Res.*, 2007, **41**(3), 620–626.
47 M. Caccin, F. Giacobbo, M. Da Ros, L. Besozzi and M. Mariani, Adsorption of uranium: cesium and strontium onto coconut shell activated carbon, *J. Radioanal. Nucl. Chem.*, 2013, **297**, 9–18.
48 S. Khandaker, T. Kuba, S. Kamida and Y. Uchikawa, Adsorption of cesium from aqueous solution by raw and concentrated nitric acid–modified bamboo charcoal, *J. Environ. Chem. Eng.*, 2017, **5**, 1456–1464.
49 C. Chen and C. J. Wang, Removal of Pb^{2+}, Ag^{+}, Cs^{+} and Sr^{2+} from aqueous solution by brewery's waste biomass, *J. Hazard. Mater.*, 2008, **151**(1), 65–70.
50 S. Dahiya, R. Tripathi and A. Hegde, Biosorption of heavy metals and radionuclide from aqueous solutions by pre-treated arca shell biomass, *J. Hazard. Mater.*, 2008, **150**(2), 376–386.

51 D. Chakraborty, S. Maji, A. Bandyopadhyay and S. Basu, Biosorption of cesium-137 and strontium-90 by mucilaginous seeds of Ocimum basilicum, *Bioresour. Technol.*, 2007, **98**, 2949–2952.

52 M. R. Awual, T. Yaita, Y. Miyazaki, D. Matsumura, H. Shiwaku and T. Taguchi, A reliable hybrid adsorbent for efficient radioactive cesium accumulation from contaminated wastewater, *Sci. Rep.*, 2016, **6**, 19937.

53 D. Ding, Z. Lei, Y. Yang, C. Feng and Z. Zhang, Selective removal of cesium from aqueous solutions with nickel(II) hexacyanoferrate(III) functionalized agricultural residue-walnut shell, *J. Hazard. Mater.*, 2014, **270**, 187–195.

54 M. R. Awual, T. Yaita, T. Taguchi, H. Shiwaku, S. Suzuki and Y. Okamoto, Selective cesium removal of radioactive liquid waste by crown ether immobilized new class conjugate adsorbent, *J. Hazard. Mater.*, 2014, **278**, 227–235.

55 D. Tang, M. Yin, X. Du, Y. Duan, J. Chen and T. Qiu, Wettability tunable conjugated microporous poly(aniline)s for long-term, rapid and ppb level sequestration of Hg(II), *Chem. Eng. J.*, 2023, **474**, 145527.

56 X. Lou, D. Tang, C. Ye, J. Chen and T. Qiu, Conjugated micro-mesoporous poly(aniline)s for ultrafast Hg(II) capture, *Sep. Purif. Technol.*, 2023, **325**, 124646.